# Experimental report

10/03/2022

**Proposal:** **5-32-934**

**Council:** 4/2021

**Title:** Correlating the Crystalline Structure with Magnetic Morphology of Magnetic Nanoparticles

**Research area:** Chemistry

**This proposal is a new proposal**

**Main proposer:** **Marianna GERINA**

**Experimental team:**
Dusan ROHAL
Dominika ZAKUTNA
Marianna GERINA
Valentina MAMELI

**Local contacts:** Nina-Juliane STEINKE

**Samples:** CoFe2O4

| Instrument | Requested days | Allocated days | From | To |
|---|---|---|---|---|
| D33 | 2 | 2 | 20/09/2021 | 22/09/2021 |

**Abstract:**

The objective of this proposal is to investigate the correlation of the magnetic morphology (using the SANSPOL) of differently shaped CoFe2O4 MNPs with their crystalline structure. SANSPOL measurements will enable us to precisely determine the chemical and magnetic morphology of MNPs with spatial resolution. The magnetization distribution through MNPs obtained by the investigation of the nuclear-magnetic interference term will unambiguously allow us to discriminate the bulk and surface contributions to the magnetic disorder. This will provide us relevant information to explain the connection between crystallinity and shape of the nanoparticles and their resulting magnetic morphology. The results of our combined approach will ultimately uncover the entanglement between the physical properties (magnetization and surface disorder) and the structure (i.e. crystalline shape and size). Revealing the correlation of the magnetic structure to the crystallinity and shape of nanoparticles is highly important for the explanation of relaxation effects, technologically relevant for e.g., magnetic hyperthermia, and the magnetic microstructure.

# Correlating the Crystalline Structure with Magnetic Morphology of Magnetic Nanoparticles

## Introduction

Magnetic nanoparticles (MNPs) reveal a peculiar magnetic property, which makes them relevant for various applications, such as in data storage, spintronics, and biomedicine. Nevertheless, the performance of the MNPs is crucially determined by surface effects. Despite the large technological importance of MNPs, the magnetic configuration and the spin distribution at the nanoparticle's surface remain a key challenge. Understanding the connection between crystalline and magnetic spin structure of MNPs is of great fundamental importance to explain the resulting macroscopic response and heating performance of MNPs [1-2]. The spin structure at the nanoparticle surface highly depends on the crystallinity of the prepared MNPs, as surface effects arise from low-coordination sites, broken exchange bonds *etc.* It is also widely accepted that there is a strong correlation between structural and magnetic disorder. Surface spin canting or disorder are indirectly accessible by Mössbauer spectroscopy[3], ferromagnetic resonance[4], and x-ray magnetic circular dichroism[5]. However, it is challenging to isolate surface-related effects from the effective magnetic anisotropy using macroscopic, integral magnetization methods. To reliably discriminate surface contribution to magnetic disorder, access to the spatially resolved magnetization is required. Half-polarized small-angle neutron scattering (SANSPOL) allows us to resolve spatially sensitive information of the spin structure with a sub-Å resolution[6]. We aim to probe the magnetization of monodisperse $CoFe_2O_4$ nanoparticles of different sizes and shapes using SANSPOL experiments and to correlate the resulting magnetic spin structure with their crystallite structure and their magnetic performance.

## Results

SANSPOL experiments were performed at the D33 instrument on 8 samples of $CoFe_2O_4$ nanoparticles (four of spherical shape and four of cubical shape) dispersed in $d_8$-toluene. Experiments were done using 5 Å neutron wavelength (with wavelength spread of $\Delta\lambda/\lambda = 10$ %). The incident neutron beam was polarized using a V-shaped polarizer, and the polarization of the neutron beam was changed with a radiofrequency spin flipper. Data were collected at detector distances of 2 and 7.8 m with collimation of 2 and 7.8 m, respectively, to cover the complete momentum transfer of interest. The neutron beam was focused on the sample using an aperture of 5x5 mm, and at the sample position, the horizontal external magnetic field was applied from 0 – 1.336 T. The collected data were processed in the Grasp software, where data were corrected for the background scattering, blocked beam, and polarization efficiency of the V-shaped polarizer (0.91) and flipper (0.99). The scattering intensity was transformed to the absolute scale by measuring the intensity of the empty beam. The pure nuclear scattering cross-section was extracted by sector analysis (20° of total opening) of the sum of I(–) and I(+) scattering cross-sections along the applied magnetic field direction (horizontal, 0°) at the highest magnetic field when the nanoparticles are magnetically saturated.

The core-shell-surfactant model was best to ascribe the measured data, where the core represents the magnetized part of the nanoparticles, the shell a non-magnetized part (dead layer), where spin disorder or canting can be present, and the surfactant corresponds to the layer of oleic acid at the nanoparticle surface. The magnetic morphology of nanoparticles was accessed from vertical sector integration (20° of total opening) of $I(-)$ and $I(+)$ scattering cross-sections. The nuclear parameters obtained from SANS and SAXS were fixed, and only the thickness of the dead layer ($d_{\text{dis}}$) and the magnetic scattering length density ($\rho_{\text{mag}}$) were refined. Figure 1 shows the SANSPOL scattering cross-section at different neutron beam polarizations with an applied magnetic field of 1.34 T for the spherical samples S3 (3.1(1) nm), S6 (6.3(2) nm), and S9 (8.6(1) nm). For each sample, there is a clear presence of magnetic contrast variation caused by varying the incident beam polarization, and the magnetic contrast is more pronounced with increasing the size of the particles. The insertions in Figure ***1*** relate to the radial distribution of $\rho_{\text{mag}}$ at different applied magnetic fields. We can see that the magnetic radius ($r_{\text{mag}}$) is clearly increasing with the applied magnetic field.

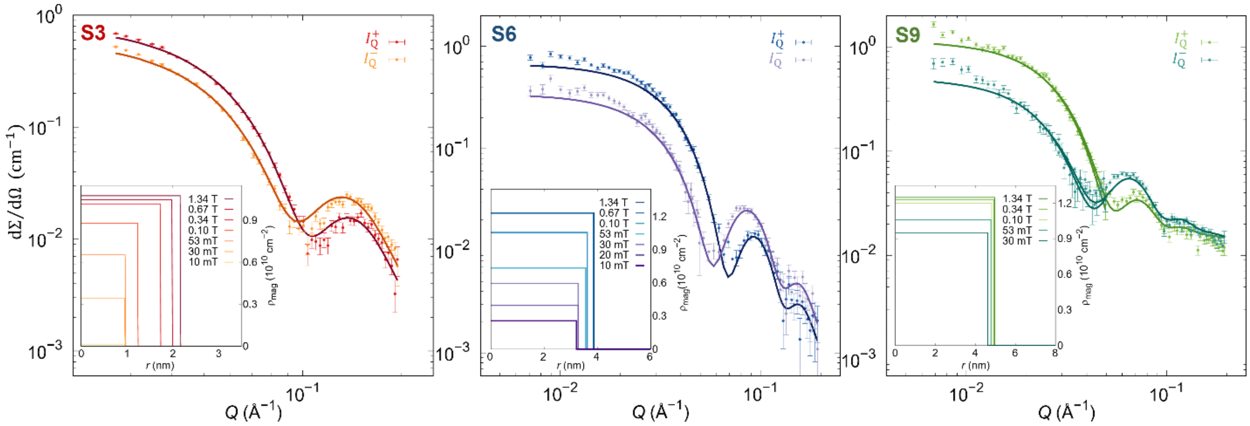

**Figure 1**: SANSPOL scattering cross section (points) at different neutron beam polarizations with applied magnetic field of 1.34 T for the spherical samples S3, S6 and S9 fitted with the model core-shell-surfactant (line). The insertions report the obtain radial distribution of $\rho_{mag}$ at different applied magnetic fields.

Obtained dependence of the $r_{mag}$ and the $d_{dis}$ on the magnetic field is visualized in Figure 2. We can see that $r_{mag}$ increases with the applied magnetic field for each sample while $d_{dis}$ decreases. For the smaller nanoparticles, S3, $r_{mag}$ gradually increases until reaching the $r_{nuc}$, suggesting that the sample is fully magnetized. In the case of larger nanoparticles (S6 and S9 samples), the increasing $r_{mag}$ with the applied magnetic field is still observed but without reaching the $r_{nuc}$, suggesting the presence of significant non-magnetized area at the nanoparticle surface corresponding either to surface spin disorder or canting. Moreover, it is clearly visible how increasing the nanoparticle size affects the total magnetized NP volume. More in-depth evaluation of data on the surface anisotropy constant and micromagnetic simulation is ongoing.

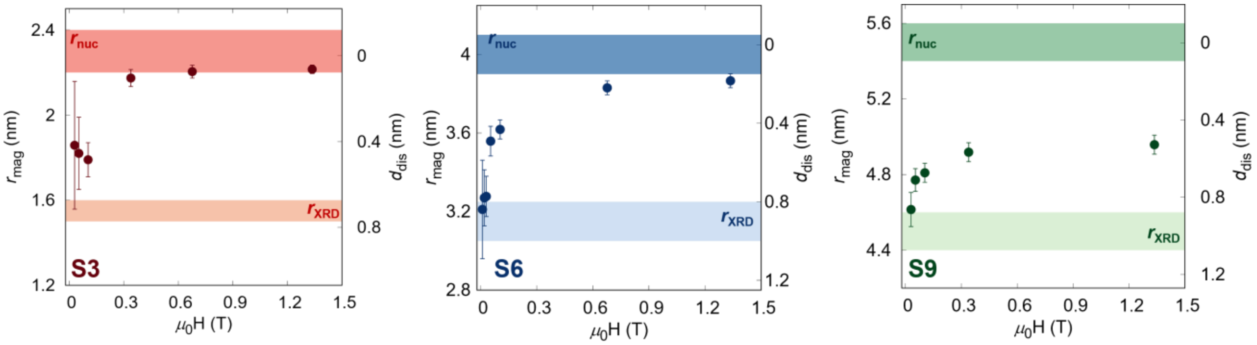

**Figure 2**: Dependence of the magnetic radius (left) and the dead layer (right) on the magnetic field for the samples S3, S6 and S9. The darker area represents the nuclear radius and the brighter the crystalline size.

## Bibliography

[1] A. Lak et al., Nano Lett. 18, 6856 (2018).
[2] A. Lappas et al., Phys. Rev. X 9, 041044 (2019).
[3] B. N.Pianciola et al., J. Magn. Magn. Mater. 377, 44 (2015).
[4] V. Bonanni et al., Appl. Phys. Lett. 112, 022404 (2018).
[5] D. S. Negi et al., Phys. Rev. B 95, 174444 (2017).
[6] D. Zákutná et al., Phys. Rev. X 10, 031019 (2020).
[7] L. Wu et al., Nano Lett. 14, 3395-3399 (2014).
[8] Le T. Lu et al., Nanoscale 7, 19596 (2015).